Dalton Transactions

Cite this: *Dalton Trans.*, 2012, **41**, 908

www.rsc.org/dalton

PAPER

A kinetics and mechanistic study on the role of the structural rigidity of the linker on the substitution reactions of chelated dinuclear Pt(II) complexes†

Allen Mambanda and Deogratius Jaganyi*

Received 11th August 2011, Accepted 5th October 2011
DOI: 10.1039/c1dt11516b

Substitution reactions of platinum complexes bearing cyclohexylamine/diamine moieties *viz.*, [Pt(H_2O)(*N*,*N*-bis(2-pyridylmethyl)cyclohexylamine)](CF_3SO_3)$_2$, **bpcHna**; [{Pt(H_2O)}$_2$-(*N*,*N*,*N*′,*N*′-tetrakis(2-pyridylmethyl)-*trans*-1,4-cyclohexyldiamine)](CF_3SO_3)$_4$, **cHn** and [{Pt(H_2O)}$_2$(*N*,*N*,*N*′,*N*′-tetrakis(2-pyridylmethyl)-4,4′-dicyclohexylmethanediamine)](CF_3SO_3)$_4$, **dcHnm** and phenylamine/diamine moieties *viz.*, ([Pt(H_2O)*N*,*N*-bis(2-pyridylmethyl)-phenylamine)](CF_3SO_3)$_2$, **bpPha**; [{Pt(H_2O)}$_2$(*N*,*N*,*N*′,*N*′-tetrakis(2-pyridylmethyl)-1,3-phenyldiamine)](CF_3SO_3)$_4$, **mPh**; [{Pt(H_2O)}$_2$(*N*,*N*,*N*′,*N*′-tetrakis(2-pyridylmethyl)-1,4-phenyldiamine)](CF_3SO_3)$_4$, **pPh** and [{Pt(H_2O)}$_2$(*N*,*N*,*N*′,*N*′-tetrakis(2-pyridylmethyl)-4,4′-diphenylmethanediamine)](CF_3SO_3)$_4$), **dPhm** with thiourea nucleophiles were studied in acidified 0.01 M $LiCF_3SO_3$ aqueous medium under pseudo-first-order conditions using stopped-flow and UV-visible spectrophotometric techniques. The rate of substitution follows a similar trend in the two sets of complexes and decreases in the order: **bpcHna** > **dcHnm** > **cHn** and **bpPha** > **dPhm** ≈ **pPh** ≈ **mPh**), respectively. The result of this study has shown that the rigidity and/or the planarity of a diamine bridge linking the two (2-pyridylmethyl)amine-chelated Pt(II) centres, influences the reactivity of the metal centres by protracting similar symmetry elements within the complexes, which determines the amount of steric influences felt on the coordination square-plane. Hence, the order of reactivity is controlled by both the steric hindrance and the magnitude of the *trans* σ-inductive effect originating from the linker towards the metal centre. These two factors also impact on the acidity of the complexes. The high negative entropies and low positive enthalpies support an associative mode of activation.

Introduction

Multinuclear Pt(II) complexes represent a novel class of compounds that have shown great potential in cancer chemotherapy.[1,2] The most well known complexes contain aliphatic diamines of variable chain lengths,[3] azines,[4] azoles,[5] 4,4′-dipyrazolylmethane[6a] and 4,4′-methylenedianiline[6b] structural groups affording terminal platinum centres possessing one or two labile ligands.

From the cytotoxic studies of multinuclear complexes,[7] it appears that the nature and in particular the length of structural motifs linking the Pt(II) coordination spheres play a pivotal structural-directing role[6] on the type of metal–DNA cross-links by introducing flexibility/rigidity of variable magnitude to their entire chemical structures. For example, an aliphatic diamine bridge introduces some flexibility in Pt–DNA cross-links[3,7] while an aromatic diamine or cycloalkyldiamine will introduce some degree of rigidity.[4,5,6a] More specifically, the cytotoxic profiles of multinuclear Pt(II) complexes with flexible alkyldiamine bridges have shown structural–activity relationships that depends on the average distance separating their Pt(II) ions.[3,8] The chain length equivalent to a 1,6-diaminohexane[3a,b] appears to be the optimum separation distance for maximum activity. Rational design of Pt(II) complexes tailored on the 1,6-diaminohexane linkers has culminated in the synthesis of BBR3464, a key tumour cytostatic with remarkable *in vitro* activity.[9] One of the factors attributed to the remarkable cytotoxicity of this trinuclear species against several tumour cells has been its ability to form a large percentage of long-range and flexible interstrand crosslinks spanning more than four nucleobases of DNA.[10]

Besides the Pt, Pt separation distance, the structural make-up of the bridge itself seems to be another important factor which controls the type of adducts formed with DNA. For example, significant differences in cytotoxicities of certain dinuclear Pt complexes can be noticed when a comparison of their antitumour activity is made between complexes of equivalent Pt, Pt separation distances, differing mainly in the chemical structures of their bridges.[11,8b,3b]

School of Chemistry, University of KwaZulu-Natal, Scottsville, 3209, South Africa

† Electronic supplementary information (ESI) available: A summary of the wavelengths used for kinetics; exemplary mass spectra for ligands **L3** and **L7**, spectral changes for the titration of **dcHnm** with NaOH; exemplary Tables of data and the respective plots showing the dependence of $k_{obs(1st/2nd)}$ on concentration of nucleophiles and temperature for some selected complexes (**bpcHna**, **dcHnm** and **pPh**). See DOI: 10.1039/c1dt11516b

Introduction of different structural fragments within the linker has also been demonstrated to modulate biological activities of multinuclear Pt(II) complexes bearing 4,4′-dipyrazolylmethane,[6a] 4,4′-methylenedianiline[6b] and mesitylene[12] bridges.

Despite all that is known about the effects of the structure of the bridging motifs on cytotoxicity, there is limited data to formulate structure–reactivity relationships between the nature of the bridging moieties of multinuclear platinum complexes and the lability of the leaving groups of the Pt(II) centres. Previous kinetics studies of Hofmann *et al.*[13a] and from our laboratory[13b] have established that substitutional reactivity of Pt dinuclears with flexible α,ω-alkyldiamine linkers is dependent on the average distance separating their Pt centres. However, the actual contribution of the bridge to the molecular mechanism of the substitution of the leaving groups remains least understood even for homologous dinuclears in which a simple structural attribute of the bridge is varied while maintaining the same structural backbone of the linker.

However, it has come out of recent kinetic studies[13a,14,15a] that the average distance separating the flexible dinuclear Pt(II) centres is not the only critical factor controlling their reactivity. For example, in a set of homologous dinuclear complexes with short aliphatic diamine bridges, a switch in the molecular symmetry from C_{2h} to C_{2v} resulted in a significant removal of the steric influences from an overlap geometry of the C_{2h} complex and at the same time promoted the 'entrapment' of the incoming nucleophiles in the C_{2v} complex.[15a] The steric relief due to the bowl molecular shape of the C_{2v} complex resulted in an unusual high substitutional reactivity. The results suggested that molecular symmetries adopted by the complexes, and maintained by the subtle differences in the structural makeup of the bridge, also control reactivity of the enjoined Pt(II) centres. In the same way, factors such as rigidity and planarity of the linker, which have potential to control the symmetry elements adopted within the entire complex, can also directly control the reactivity of the Pt atoms in multinuclear complexes.

In this study, a total of five dinuclear complexes as well as their two mononuclear analogues were synthesized and their ligand substitution reactions studied with thiourea nucleophiles in acidified (pH 2.0) lithium triflate {$Li(CF_3SO_3)$} aqueous medium. Two of the dinuclear complexes are linked by diamine bridges bearing cyclohexyl fragments while the other three are linked by bridges containing phenylenic moieties. This work seeks to extend our understanding of the role of the diamine bridge on the reactivity of the dinuclear complexes when variable structural rigidity as well as planarity is introduced in the structural backbone of diamine bridges.

Experimental

Materials and reagents

All synthetic reactions were performed under an inert atmosphere of nitrogen. All reagents were used as supplied. The diamines were procured from Fluka. 2-(Chloromethyl)pyridine hydrochloride, sodium perchlorate monohydrate ($NaClO_4·H_2O$), silver perchlorate ($AgClO_4$, 99.9%) and the thiourea nucleophiles were purchased from Aldrich. Potassium tetrachloroplatinate (K_2PtCl_4, 99.99%) was purchased from Strem Chemicals. Ultrapure water (Modulab System) was used for all aqueous reactions.

Preparation of ligands

The ligands synthesized for this investigation were *N*,*N*-bis(2-pyridylmethyl)cyclohexylamine (**L1**); *N*,*N*,*N*′,*N*′-tetrakis(2-pyridylmethyl)-*trans*-1,4-cyclohexyldiamine (**L2**); *N*,*N*,*N*′,*N*′-tetrakis(2-pyridylmethyl)-4,4′-dicyclohexylmethanediamine (**L3**). *N*,*N*′-bis(2-pyridylmethyl)phenylamine (**L4**); *N*,*N*,*N*′,*N*′-tetrakis(2-pyridylmethyl)-1,3-phenyldiamine (**L5**); *N*,*N*,*N*′,*N*′-tetrakis(2-pyridylmethyl)-1,4-phenyldiamine (**L6**) and *N*,*N*,*N*′,*N*′-tetrakis(2-pyridylmethyl)-4,4′-diphenylmethanediamine (**L7**).

The procedure of Sato *et al.*[16] was adapted for the synthesis of ligands **L1–L3** based on the report of Toftlund[18] described for the 1,2-diaminocyclohexane derivative. A procedure described by Karlin and co-workers[17] for the tris[(2-pyridyl)methyl]amine derivative was followed for the preparation of **L4**. Ligand **L5** was prepared following the procedures of Schindler *et al.*[19b] while the procedure of Buchen *et al.*[19a] was used to prepare the ligands **L6** and **L7** with some minor modifications in their final purification steps. For the purification of all the ligands with an aromatic core, it was necessary to elute the concentrated organic layers through a chromatographic column packed with 2 g of activated charcoal, 5 g neutral alumina and sodium sulfate using chloroform as a solvent to collect light yellow coloured solutions. On concentrating the chloroform fractions, **L4** yielded an orange oil while **L6** precipitated out as beige flakes. **L5** precipitated from the slow evaporation of its ethanolic solution as an off-white powder while **L7** precipitated out from its diethyl ether solution. Recrystallization of the crude powders from their hot solutions {ethanol–acetone (19 : 1) mixture for **L5** and **L6**} and ether for **L7** afforded pure compounds.

All the synthesized ligands were characterized by microanalysis (except for **L4** which was obtained as an oil); NMR and TOF MS ES$^+$. Exemplary mass spectra for **L3** and **L7** are shown in Figures SI 1a and 1b (ESI†), respectively.

L1. Yield: 1342 mg (40%), white powder. ^{1}H NMR (400 MHz, $CDCl_3$) δ (ppm): 8.58 (d, 2H), 8.50–7.60 (m, 4H), 7.05 (t, 2H), 3.39 (s, 4H), 2.55 (m, 1H), 1.90 (d, 2H), 1.8 (m, 2H), 1.60 (d, 2H), 1.35 (m, 2H), 1.19 (m, 2H). ^{13}C NMR (100 MHz, $CDCl_3$) δ (ppm): 27.0, 29, 57.0, 60.5, 122.0, 123.0, 136.0, 148.0, 161. IR (KBr, 4000–400 cm^{-1}) $\bar{\nu}$: 2958–2854 (alkyl C–H stretch), 1589 C=N (pyridyl). Anal. Calc. for $C_{18}H_{23}N_3$: C, 76.81; H, 8.24; N, 14.93. Found: C, 76.8; H, 8.18; N, 14.89%. MS-ES$^+$, *m*/*z*: 282.2069, (M + 1)$^+$.

L2. Yield: 1276 mg (44%), white powder. ^{1}H NMR (400 MHz, $CDCl_3$) δ (ppm): 8.60 (t, 4H), 7.50–7.60 (m, 8H), 7.10 (t, 4H), 3.95 (s, 8H), 2.35 (m, 2H), 2.10 (m, 4H), 1.4 (m, 4H). ^{13}C NMR (100 MHz, $CDCl_3$) δ (ppm): 27, 47, 56, 60, 122.0, 123.0, 136, 149.0, 158.0. IR (KBr, 4000–400 cm^{-1}) $\bar{\nu}$: 2958–2854 (alkyl C–H stretch), 1589 (C=N, pyridyl). Anal. Calc. for $C_{30}H_{34}N_6$: C, 75.28; H, 7.16; N, 17.56. Found: C, 75.29; H, 7.10; N, 17.45%. MS-ES$^+$ *m*/*z*: 479.2973 M + 1)$^+$

L3. Yield: 1519 mg (44%), off-white powder. ^{1}H NMR (400 MHz, $CDCl_3$) δ (ppm): 8.62 (t, 4H), 7.50–7.65 (m, 8H), 7.10 (t, 4H), 3.95 (s, 8H), 2.45 (t, 2H), 1.95 (d, 4H), 1.70 (m, 4H), 1.48 (q, 2H), 1.25 (m, 4H), 1.15 (t, 2H), 1.0 (m, 4H). ^{13}C NMR (100 MHz, $CDCl_3$) δ (ppm): 28.0, 33.2, 34.0, 44,0, 57.5, 60.0, 122.0, 123.0,

136.5, 148.0, 162.0. IR (KBr, 4000–400 cm^{-1}) $\bar{\nu}$: 2958–2854 (alkyl C–H stretch), 1589 (C═N, pyridyl). Anal. Calc. for $C_{37}H_{46}N_6$: C, 77.31; H, 8.07; N, 14.62. Found: C, 77.28; H, 8.26; N, 14.41%. MS-ES$^+$ m/z: 575.3862 $(M + 1)^+$.

L4. Yield: 2507 mg (71%), bright orange oil. ^{1}H NMR (400 MHz, $CDCl_3$) δ (ppm): 8.58 (d, 2H), 7.7 (t, 2H), 7.65 (dt, 4H), 7.60 (t, 1H), 7.20 (m, 2H), 6.7 (m, 2H), 4.50 (s, 4H). ^{13}C NMR (100 MHz, $CDCl_3$) δ (ppm) 57.0, 113, 117, 122, 123, 129, 138, 147, 150, 165. IR (KBr, 4000–400 cm^{-1}) $\bar{\nu}$: 2958–2854 (alkyl C–H stretch), 1589 (C═N, pyridyl). MS-ES$^+$, m/z: 276.1501, $(M + 1)^+$.

L5. Yield: 1006 mg (35%), off-white powder. ^{1}H NMR (400 MHz, $CDCl_3$) δ (ppm): 8.62 (d, 4H), 8.29 (t, 4H), 7.85 (d, 4H), 7.75 (t, 4H), 6.0 (m, 4H), 5.60 (s, 8H). ^{13}C NMR (100 MHz, $CDCl_3$) δ (ppm): 59.0, 112, 113, 122.0, 123.0, 128.0, 136.5, 141.0, 150.0, 162.0. IR (KBr, 4000–400 cm^{-1}) $\bar{\nu}$: 2958–2854 (alkyl C–H stretch), 1589 (C═N, pyridyl). Anal. Calc. for $C_{30}H_{28}N_6$: C, 76.24; H, 5.97; N, 17.78. Found: C, 76.28; H, 5.97; N, 17.53%. MS-ES$^+$ m/z: 473.2468 $(M + 1)^+$

L6. Yield: 1365 mg (48%), beige flakes. ^{1}H NMR (400 MHz, $CDCl_3$) δ (ppm): 8.65 (d, 4H), 8.29 (t, 4H), 7.85 (d, 4H), 7.75 (t, 4H), 6.0 (m, 4H) 5.60 (s, 8H). ^{13}C NMR (100 MHz, $CDCl_3$) δ (ppm): 59.0, 113, 122.0, 123.0, 136.5, 141.0, 150.0, 162.0. IR (KBr, 4000–400 cm^{-1}) $\bar{\nu}$: 2958–2854 (alkyl C–H stretch), 1589 (C═N, pyridyl). Anal. Calc. for $C_{30}H_{28}N_6$: C, 76.24; H, 5.97; N, 17.78. Found: C, 76.26; H, 5.85; N, 17.86%. MS-ES$^+$ m/z: 473.2454 $(M + 1)^+$

L7. Yield: 1123 mg (33%), off-white powder. ^{1}H NMR (400 MHz, $CDCl_3$) δ (ppm): 8.60 (d, 4H), 7.60 (t, 4H), 7.35 (d, 4H), 7.20 (t, 4H), 7.0 (m, 4H), 6.6 (m, 4H), 4.8 (s, 8H), 4.45 (s, 2H). ^{13}C NMR (100 MHz, $CDCl_3$) δ (ppm): 41, 57, 112, 113, 122.0, 123.0, 128.0, 136.0, 150.0, 158.0. IR (KBr, 4000–400 cm^{-1}) $\bar{\nu}$: 2958–2854 (alkyl C–H stretch), 1589 (C═N, pyridyl). Anal. Calc. for $C_{37}H_{34}N_6$: C, 78.97; H, 6.09; N, 14.95. Found: C, 78.55; H, 6.13; N, 14.62%. MS-ES$^+$ m/z: 563.2923 $(M + 1)^+$.

Synthesis of Pt(II) complexes

The two mononuclear and the dinuclear Pt(II) complexes listed below (**1–7**) were synthesized starting from ligands **L1–L7**, following a literature procedure.[13a] The complexes were characterized by NMR, IR and microanalysis. These were [Pt(Cl)(*N*,*N*-bis(2-pyridylmethyl)cyclohexylamine)](ClO_4) (**1**); [{Pt(Cl)}$_2$(*N*,*N*,*N*′,*N*′-tetrakis(2-pyridylmethyl)-*trans*-1,4-cyclohexyldiamine)](ClO_4)$_2$ (**2**); [{Pt(Cl)}$_2$(*N*,*N*,*N*′,*N*′-tetrakis(2-pyridylmethyl)-4,4′-dicyclohexylmethanediamine)](ClO_4)$_2$ (**3**); [Pt(Cl)(*N*,*N*-bis(2-pyridylmethyl)phenylamine)](ClO_4) (**4**); [{Pt-(Cl)}$_2$(*N*,*N*,*N*′,*N*′-tetrakis(2-pyridylmethyl)-1,3-phenyldiamine)]-(ClO_4)$_2$ (**5**); [{Pt(Cl)}$_2$(*N*,*N*,*N*′,*N*′-tetrakis(2-pyridylmethyl)-1,4-phenyldiamine)](ClO_4)$_2$ (**6**); [{Pt(Cl)}$_2$(*N*,*N*,*N*′,*N*′-tetrakis-(2-pyridylmethyl)-4,4′-diphenylmethanediamine)](ClO_4)$_2$ (**7**).

1. Yield: 207.8 mg (47%). ^{1}H NMR (400 MHz, DMF-d_7) δ (ppm): 9.05 (d, 2H), 8.40 (t, 2H), 7.95 (d, 2H), 7.80 (t, 2H), 5.45 (d, 2H), 5.35 (d, 2H), 3.05 (m, 1H), 2.35 (m, 2H), 1.7 (m, 2H) 1.2 (m, 6H). ^{13}C NMR (125 MHz, DMF-d_7) δ (ppm): 24.5, 25.0, 30.0, 66.0, 73, 123.0, 126.0, 142.0, 149.0, 168. ^{195}Pt NMR (85 MHz, DMF-d_7) δ (ppm): –2335. IR (KBr, 4000–300 cm^{-1}) $\bar{\nu}$: 2958–2854 (alkyl C–H stretch), 1589 (C═N, pyridyl), 1090–1100 (perchlorate counter ion), 324–330 (Pt–Cl stretch). Anal. Calc. for $PtC_{18}H_{23}N_3Cl_2O_4$: C, 35.36; H, 3.79; N, 6.94. Found: C, 35.36; H, 3. 83; N, 6.92%.

2. Yield: 169.7 mg (41%). ^{1}H NMR (400 MHz, DMF-d_7) δ (ppm): 8.90 (d, 4H), 8.3 (t, 4H), 8.4 (d, 4H), 7.75 (t, 4H), 5.2 (d, 4H), 5.30 (d, 4H), 2.35 (m, 2H), 2.10 (m, 4H), 1.5 (m, 4H). ^{13}C NMR (125 MHz, DMF-d_7) δ (ppm): δ (ppm): 58, 60, 122.0, 123.0, 136, 149.0, 158.0. ^{195}Pt NMR (85 MHz, DMF-d_7) δ (ppm): –2330. IR (KBr, 4000–300 cm^{-1}) $\bar{\nu}$: 2958–2854 (alkyl C–H stretch), 1589 (C═N, pyridyl), 1090–1100 (perchlorate counter ion), 324–330 (Pt–Cl stretch). Anal. Calc. for $Pt_2C_{30}H_{34}N_6Cl_4O_8$: C, 31.64; H, 3.01; N, 7.38. Found: C, 31.63; H, 3.06; N, 7.36%.

3. Yield: 177.4 mg (40%). ^{1}H NMR (400 MHz, DMF-d_7) δ (ppm): 9.05 (d, 4H), 8.42 (t, 4H), 7.95 (d, 4H), 7.79 (t, 4H), 5.38 (d, 4H), 5.29 (d, 4H), 3.0 (m, 2H), 2,45 (m, 4H), 1,8 (m, 4H), 1.59 (m, 4H), 1.4 (m, 2H), 1.0 (m, 6H). ^{13}C NMR (100 MHz, DMF-d_7) δ (ppm): 23.0, 52.5, 55.0, 127.1, 128.0, 128.0, 145.0, 148.0, 164.0. ^{195}Pt NMR (107 MHz, DMF-d_7) δ (ppm): –2320. IR (KBr, 4000–300 cm^{-1}) $\bar{\nu}$: 2958–2854 (alkyl C–H stretch), 1589 (C═N, (pyridyl), 1090–1100 (perchlorate counter ion), 324–330 (Pt–Cl stretch). Anal. Calc. for $Pt_2C_{37}H_{46}N_6Cl_4O_8$: C, 35.99; H, 3.75; N, 6.81. Found: C, 35.90; H, 3.73; N, 6.64%.

4. Yield: 245.9 mg (56%). ^{1}H NMR (400 MHz, DMF-d_7) δ (ppm): 9.10 (d, 2H), 8.30–8.40 (t, d merged, 4H), 7.85 (d, 2H), 7.75 (m, 2H), 7.5 (m, 2H), 7.35 (m, 1H) 5.7 (d, 2H), 6.0 (d, 2H). ^{13}C NMR (100.6 MHz, DMF-d_7) δ (ppm): 71.0, 124.0, 125.0, 127, 130, 136.0, 142, 149.5, 150, 166. ^{195}Pt NMR (107.2 MHz, DMF-d_7) δ (ppm): –2300. IR (KBr, 4000–300 cm^{-1}) $\bar{\nu}$: 2958–2854 (alkyl C–H stretch), (1589 (C═N, pyridyl), 1090–1100 (perchlorate counter ion), 324–330 (Pt–Cl stretch). Anal. Calc. for $PtC_{18}H_{17}N_3Cl_2O_4$: C, 35.72; H, 2.83; N, 6.94. Found: C, 35.83; H, 2.79; N 6.92%.

5. Yield: 190.0 mg (47%). ^{1}H NMR (400 MHz, DMF-d_7) δ (ppm): 8.95 (d, 4H), 8.25 (t, d, 6H), 7.85 (m, 4H), 7.75 (t, s (merged), 6H), 6.0 (d, 4H) 5.60 (d, 4H). ^{13}C NMR (125 MHz, DMF-d_7) δ (ppm): 58.0, 113, 122.0, 123.0, 136.5, 141.0,150.0, 162.0. ^{195}Pt NMR (107 MHz, DMF-d_7) δ (ppm): –2312. IR (KBr, 4000–300 cm^{-1}) $\bar{\nu}$: 2958–2854 (alkyl C–H stretch), 1589 (C═N, pyridyl), 1090–1100 (perchlorate counter ion), 324–330 (Pt–Cl stretch). Anal. Calc. for $Pt_2C_{30}H_{28}N_6Cl_4O_8$: C, 31.81; H, 2.49; N, 7.42. Found: C, 31.84; H, 2.47; N, 7.39%.

6. Yield: 215.6 mg (53%). ^{1}H NMR (400 MHz, DMF-d_7) δ (ppm): 9.02 (d, 4H), 8.55 (m, 8H), 8.25 (m, 4H), 7.95 (m, 4H), 6.0 (d, 4H) 5.60 (d, 4H). ^{13}C NMR (125 MHz, DMF-d_7) δ (ppm): 59.0, 113, 122.0, 123.0, 136.5, 141.0, 150.0, 162.0. ^{195}Pt NMR (107 MHz, DMF-d_7) δ (ppm): –2315. IR (KBr, 4000–300 cm^{-1}) $\bar{\nu}$: 2958–2854 (alkyl C–H stretch), 1589 (C═N, pyridyl), 1090–1100 (perchlorate counter ion), 324–330 (Pt–Cl stretch). Anal. Calc. for $Pt_2C_{30}H_{28}N_6Cl_4O_8$: C, 31.81; H, 2.49; N, 7.42. Found: C, 31.79; H, 2.46; N, 7.32%.

7. Yield: 152.2 mg (34%). ^{1}H NMR (400 MHz, DMF-d_7) δ (ppm): 9.05 (d, 4H), 8.60 (t, 4H), 7.95 (d, 4H), 7.85 (t, 4H), 7.5 (m, 4H), 7.2 (m, 4H), 5.4 (d, 4H), 5.3 (d, 4H), 4.2 (s, 2H). ^{13}C NMR (100 MHz, $CDCl_3$) δ (ppm): 41, 57, 112, 113, 122.0, 123.0, 128.0, 136.0, 150.0, 158.0. IR (KBr, 4000–300 cm^{-1}) $\bar{\nu}$: 2958–2854 (alkyl C–H stretch), 1589 (C═N, pyridyl), 1090–1100 (perchlorate counter ion), 324–330 (Pt–Cl stretch). Anal. Calc. for $Pt_2C_{37}H_{34}N_6Cl_4O_8$: C, 36.34, H, 2.80; N, 6.87. Found: C, 36.41; H, 2.80; N, 6.77%.

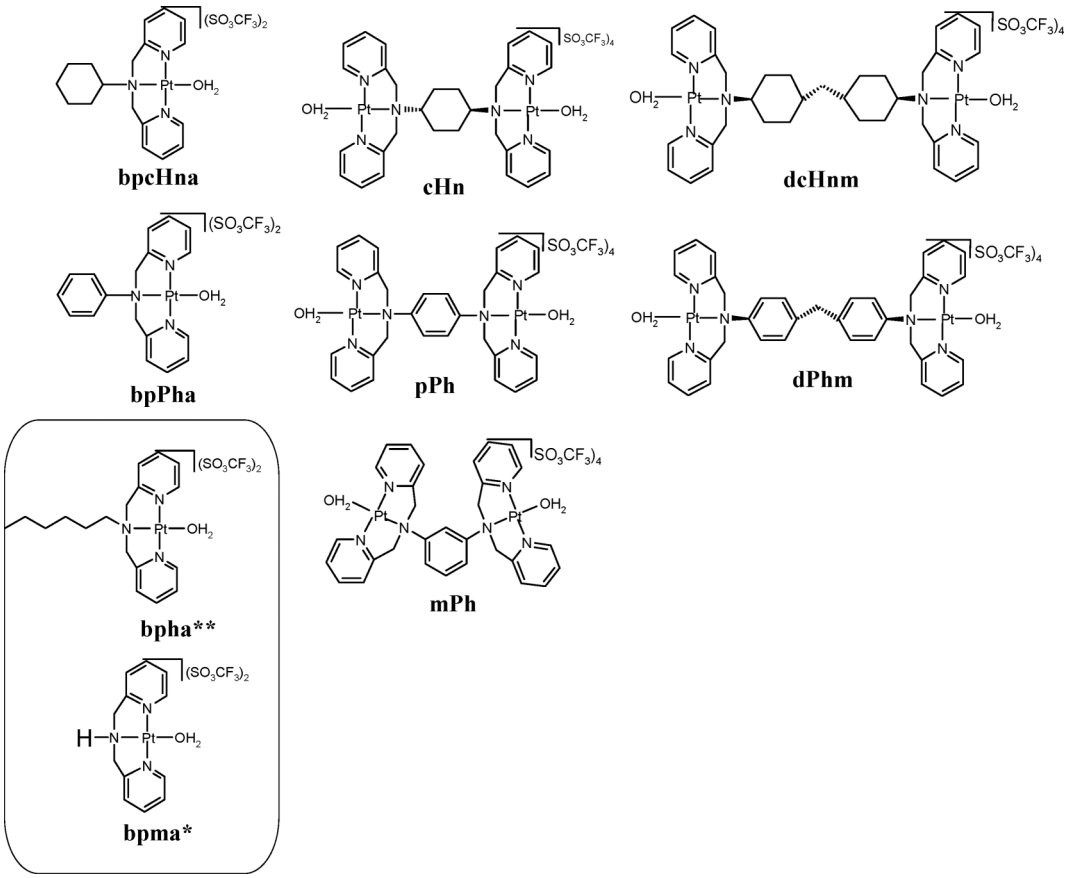

Fig. 1 Structures of dinuclear Pt(II) complexes and their respective mononuclear analogues synthesized in this study. Rectangular inset: Structures of additional mononuclear complexes included for comparison purposes. Their kinetic data was adapted from ref. 15*a** and 15*b*****, respectively.

Kinetic measurements and computational details

Preparation of aqueous solutions of Pt(II) complexes. The structures of the aqua derivatives used in the kinetics experiments are shown in Fig. 1. The aqueous solutions of the complexes were prepared from their respective chloro derivatives following a literature procedure by Bugarčić *et al.*[20a] The aqua complexes investigated were $[Pt(H_2O)(N,N$-bis(2-pyridylmethyl)cyclohexylamine$)](CF_3SO_3)_2$ (**bpcHna**); $[\{Pt(H_2O)\}_2(N,N,N',N'$-tetrakis(2-pyridylmethyl)-*trans*-1,4-cyclohexyldiamine$)](CF_3SO_3)_4$ (**cHn**); $[\{Pt(H_2O)\}_2(N,N,N',N'$-tetrakis(2-pyridylmethyl)-4,4′-dicyclohexylmethanediamine$)](CF_3SO_3)_4$ (**dcHnm**). $[Pt(H_2O)(N,N$-bis(2-pyridylmethyl)phenylamine$)](CF_3SO_3)_2$ (**bpPha**); $[\{Pt(H_2O)\}_2(N,N,N',N'$-tetrakis(2-pyridylmethyl)-1,3-phenyldiamine$)](CF_3SO_3)_4$ (**mPh**); $[\{Pt(H_2O)\}_2(N,N,N',N'$-tetrakis(2-pyridylmethyl)-1,4-phenyldiamine$)](CF_3SO_3)_4$ (**pPh**) and $[\{Pt(H_2O)\}_2(N,N,N',N'$-tetrakis(2-pyridylmethyl)-4,4′-diphenylmethanediamine$)](CF_3SO_3)_4$, (**dPhm**).

Solutions of the nucleophiles *viz*. thiourea (tu), *N*,*N*′-dimethylthiourea (dmtu) and *N*,*N*,*N*′,*N*′-tetramethylthiourea (tmtu) were prepared by dissolving appropriate amounts of the nucleophiles in a solution of pH 2.0, whose ionic strength had been adjusted to 0.02 M using $LiSO_3CF_3$. The stock solution of each nucleophile, of concentration approximately equal to 100-fold over that of the dinuclear complexes or 50-fold over that of the monomeric complexes (**bpPha** and **bpcHna**) was diluted with a 0.02 M ionic strength solution to afford serial concentrations which are at least 20-fold (for dinuclears) and 10-fold excess (mononuclears) over that of the metal complexes. These concentrations of the nucleophiles were chosen to maintain pseudo-first-order conditions during the course of the experiments. This also forced the reactions to go to completion.

Instrumentation and spectrophotometric measurements. A Bruker Avance DPX 400 NMR spectrometer and a Carlo Erba Elemental Analyzer 1106 were used to confirm the identity and purity of both the ligands and complexes. Infrared spectra of all the compounds were recorded in the range 4000–300 cm^{-1} on a Spectrum One FT-IR as KBr pellets. The spectral data of the mass of ligands were acquired by a Micromass TOF MS operated in a positive ion mode. UV-visible spectra and kinetic measurements of slow reactions were recorded on a Cary 100 Bio UV-visible spectrophotometer with a cell compartment thermostated by a Varian Peltier temperature controller having an accuracy of ± 0.05 °C. The pH measurements were recorded on a Jenway 4330 pH meter with a combined Jenway glass microelectrode which had been calibrated with standard buffer solutions of pH 4.0, 7.0 and 10.0 (Merck). The KCl solution in the reference electrode was replaced with a 3 M NaCl electrolyte to prevent precipitation of KSO_3CF_3 during use.[20b] Kinetic measurements of the first and fast reaction steps were monitored on an Applied Photophysics

SX.18 MV (v4.33) stopped-flow reaction analyzer coupled to an online data acquisition system. The temperature of the instrument was controlled to within ± 0.1 °C.

Density functional theoretical (DFT)[21] calculations were performed with the Spartan '04 for Windows quantum chemical package[22] using the B3LYP[23] method, utilizing the LACVP+**[24] pseudopotentials basis set. The dinuclear and the monomeric complexes were all modeled as cations of a total charge of +4 and +2, respectively.

Results and discussion

Acidity of the aqua Pt(II) complexes

A typical plot of the UV-visible spectra acquired during the course of the titration of the complexes with NaOH is shown in Fig. 2 for **bpPha**.

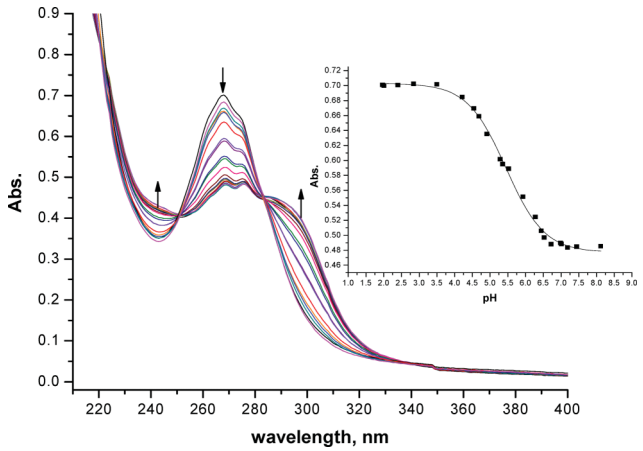

Fig. 2 UV-visible spectra for the titration of 0.1 mM **bpPha** with NaOH, pH range 2–9, T = 298 K. Inset is the titration curve at 270 nm.

In the acidic range, the spectra of all the dinuclear complexes and the two mononuclear complexes are characterized by sharp absorption bands (refer also to Figure SI 2 (ESI†) for the titration spectra of **dcHnm**). All compounds had absorption bands within a narrow range of 267–270 nm with discernable red-shifted shoulders within the 275–278 nm wavelength range. The major absorption bands for all the complexes are quite similar in shape and comparable to those reported[25] for the flexible α,ω-alkyldiamine-bridged dinuclears[15a] and the reference mononuclear complex, [Pt(H$_2$O)(*N*,*N*-bis(2-pyridylmethyl)amine](CF$_3$SO$_3$)$_2$] (**bpma**) under similar prevailing conditions. Upon adding the titrant (NaOH) the absorption bands in the 267–270 nm range gradually decrease (in the direction indicated by the central arrow in Fig. 2) while the red-shifted shoulders remain almost constant. Another broader shoulder peak appears in the wavelength range 300–305 nm during the course of the titration as hydroxo species of the complexes are formed. When the titration data which is taken at a single wavelength within the 267–270 nm peaking range is fitted to the standard Boltzmann equation, the pK_a values for the deprotonation of the coordinated aqua ligands are obtained. The results are summarized in Table 1.

The pK_a values and Fig. 2 indicate that at the pH of 2.0 (0.01 M CF$_3$SO$_3$H solution) at which the kinetics of reactions were studied, all the complexes exist as their aqua forms. The aqua species are regenerated from the hydroxo species when titrated with triflic acid with no observed shifts in the baseline as well as the isosbestic points.

Data in Table 1 reveals a similar trend observed for the aliphatic diamine-bridged analogues from our previous work.[15a] The deprotonation of the first aqua ligand of each dinuclear complex occurs at pH values that are about one to two units lower than the values at which the second aqua ligands are deprotonated. For example, the pK_{a1} values of **cHn** (4.4 ± 0.2) and **dcHnm** (4.6 ± 0.1) are relatively lower than their monomeric analogue **bpcHna** (5.6 ± 0.2) by about one pH unit. However, Pt, Pt separation distance as introduced by a methylene spacer in **dcHnm** did not result in significant change in the basicity of the aqua ligands relative to **cHn**. The pK_{a2} values of **cHn** (5.6 ± 0.2) and **dcHnm** (5.7 ± 0.02) are both comparable to the pK_a values of **bpcHna** (5.6 ± 0.2), indicating the stepwise nature of the deprotonation process in all the dinuclear complexes.

When the comparison is extended to complexes with phenyl groups, similar trends are noted. The deprotonation of the first aqua ligands of **pPh**; **mPh** and **dPhm** occurs at pH values that are more than one pH unit lower than for the second deprotonation steps. The pK_a value of the monomeric **bpPha** (5.4 ± 0.2) is higher than the pK_{a1} values of **pPh** (3.3 ± 0.1); **mPh** (3.2 ± 0.1) and **dPhm** (4.1 ± 0.03), indicating increased acidity of the coordinated aqua ligands upon forming the dinuclear complexes. The increase in acidity of symmetrical dinuclear Pt(II) aqua complexes has been reported[13a,26] before and ascribed to charge addition. A similar comparison between the pK_{a2} values for **pPh** (5.2 ± 0.1); **mPh** (5.1 ± 0.1) and **dPhm** (5.3 ± 0.3) and the pK_a values of **bpPha** (5.7 ± 0.2) signifies again the stepwise nature in the deprotonation process of the aromatic bridged complexes.

When the pK_a data for respective complexes with cyclohexyl moieties are compared to their analogues bearing aromatic structural moieties, a trend is observed. The pK_a values of the latter complexes (bridged by moieties which have sp^2-hybridized carbon frameworks) are slightly lower than the former complexes (bridged by moieties which have sp^3-hybridized carbon frameworks). This can be due to a more efficient delocalization of charge within the bridging frameworks of the latter complexes, which makes the

Table 1 Summary of pK_a data obtained for the deprotonation of Pt(II)-bound aqua ligands (within pH range 2–9), using NaOH as titrant

	bpma	bpcHna	cHn	dcHnm	bpPha	mPh	pPh	dPhm
pK_{a1}	5.5 ± 0.2[a]	5.6 ± 0.2	4.4 ± 0.2	4.6 ± 0.1	5.4 ± 0.2	3.2 ± 0.1	3.3 ± 0.1	4.1 ± 0.03
pK_{a2}			5.6 ± 0.2	5.7 ± 0.02		5.1 ± 0.1	5.2 ± 0.1	5.3 ± 0.3

The data from the titrations were fitted either to equation, $y = a + (b - a)/(1 + 2.718((x - pK_{a1}/m) + (c - b)/(1 + 2.718((x - pK_{a2})/n))$, for measuring two p$K_a$ values or the Boltzmann equation, $y = A_2 + (A_1 - A_2)/(1 + \exp((x - x_0)/dx)$ for measuring one pK_a value using the Origin 7.5® program.[a] Data from ref. 39.

Pt centres of the aromatic bridged complexes more electrophilic, leading to increased acidification of their aqua leaving groups. However, it is also known[27] that phenyldiamines are slightly poorer σ-donors than cycloalkyldiamines. Thus, the positive inductive effects due to the cyclohexyldiamine bridge or pendant, makes deprotonation of the coordinated aqua ligand difficult by lowering the electrophilicity of the Pt atoms, resulting in increased basicity.[28] This thinking is supported by looking at the pK_a values of **bpcHna** *vs*. **bpPha**. Similar results have been reported in a recent study by Eldik *et al.*[26] The shorter and conjugated buta-1,3-diyne bridge caused the *cis*-coordinated aqua leaving groups of the [Pt(DACH)(H_2O)$_2$] (DACH = 1,2-diaminocyclohexane) headgroups to deprotonate at lower pH values when compared to their aliphatic-bridged counterparts.

Computational calculations

Table 2 shows the geometry-optimized structures and the location of the frontier molecular orbitals. An extract of key geometric data from the DFT[21] calculations is summarized in Table 3.

A look at the calculated structures of the dinuclear complexes reveals a general pattern between the number of carbon atoms making the shortest connecting link between the nitrogen atoms of the diamine bridge, *n*, and the shape adopted by the chelated dinuclear Pt(II) complexes. If *n* is odd, the dinuclear complex is bowl or trough-shaped and falls in a C_{2v} point group while an even number of carbon atoms in the connecting fragment results in a slip-up structure belonging to the C_{2h} point group symmetry. For example, the four carbon atoms making the shortest connecting link between the *n* atoms in the *trans*-1,4-diaminocyclohexane linker fragment lends a slip-up overlap geometry of the C_{2h} point group symmetry on the structure of **cHn**. The structure of this complex is similar to the flexible α,ω-alkyldiamines dinuclears with an even number of carbon atoms in their bridges, reported in our previous work.[15a]

When a methylene spacer is incorporated to join two **bpcHna** complexes *via* their pendants, the resultant complex assumes a trough-shaped bowl structure. The structure of the **dcHnm** complex falls into a C_{2v} point group symmetry, derived from a connecting framework of nine carbon atoms between the *n* atoms of the diamine linker. Due to the moderate flexibility of the diaminocyclohexane rings, the nine carbon atoms forming the linking fragments of the 4,4′-dicyclohexylmethanediamine bridge connect two enjoined cyclohexyl rings' frames in a helical fashion. Thus, the helical conformation of the linker atoms maintains a perfect trough-shaped structure at the Pt chelates. This structure is relatively free from the aerial steric hindrance that is possible in the C_{2h} structure of **cHn**. However, its overlooking coordination planes make a large hinge angle of 143° at the carbon atom of the central methylene spacer in the bridge. Thus, its cavity is relatively shallow in depth and has a wider basal separation distance.

A comparison between the calculated structures of the isomeric dinuclears, **mPh** and **pPh** is instructive on the aforesaid relationship between the number of carbon atoms in their connective diamine bridges, *n*, and the symmetry elements and hence the molecular structures adopted by the Pt complexes. In the isomeric **mPh** and **pPh** complexes, the phenyl bridging framework comprises three and four carbon atoms, respectively, resulting in two different theoretical molecular structures. Thus, **pPh** (n = 4) has a C_{2h} slip-up overlap geometry similar to **cHn** and other even-bridged dinuclears[15a] while the **mPh** complex (n = 3) has bowl-shaped structure of the C_{2v} point group symmetry. A similar symmetry-to-molecular shape relationship is noticed in the crystal structures of 3,6-bis{*trans*-Pt(PEt_3)$_2$(NO_3)$_2$}-9,10-bis(hexacyloxyl-; dodecyloxyl-)phenanthrene,[29] two dinuclear Pt(II) complexes with a common phenanthrene bridge. Their three conjugated and angular rings of the phenanthrene bridge, forces bowl molecular structures in the complexes.

As in the structure of the **dcHnm**, the diamine bridge of the **dPhm** complex comprises two phenyl rings separated by an incorporated methylene spacer. The two phenyl rings and a methylene-carbon spacer make a total of nine carbon atoms within the shortest link of carbon atoms making up the 4,4′-diphenylmethanediamine bridge. A trough-shaped structure belonging to a C_{2v} point-group symmetry is expected. However, its DFT[21]-structure turns out to be a heavily distorted trough. The Pt coordination planes are orientated in a twisted anti-conformation relative to each other. To understand the origin of the conformational distortion in the structure of **dPhm** one need to consider that the pyridyl rings of the chelate headgroups must maintain an in-plane coordination geometry at the metal centre so as to maintain an efficient removal of electron density through π-back bonding[28] from the filled 5d orbitals on the Pt metal centres to the pyridyl π-acceptor ligands of the chelate headgroups. However, an in-plane geometry of the pyridyl rings at the headgroups creates structural constrains at the two square-coordination planes which can be relieved by concomitant reorganization within the linker piece. The distortion is a necessary reorganization extended beyond the linker framework, mediated both by the rigidity of the planar phenyl rings as well as the flexibility of the methylene carbon spacer. As a result, rotation is only possible on the central methylene carbon, forcing a sheer-twist on its chelate headgroups. Thus, the two enjoined aromatic rings lie in almost perpendicular planes. The sheer-twisted overlooking coordination planes of this distorted trough-shaped complex make a hinge angle of 135° at the central carbon atom of the methylene spacer of the linker. Thus, the distorted trough is relatively shallow in depth and has a wider basal separation distance similar to that of **dcHnm**. As will be discussed shortly, the structural features of the diamine linkers and their steric influences at the Pt square-planes of these complexes appear to be the major factors controlling the reactivity of their substitution reactions with incoming nucleophiles.

Kinetic measurements

Spectral changes accompanying the reactions between the complexes and nucleophiles (tu, dmtu, tmtu) were recorded over the 200–600 nm wavelength range to establish suitable wavelengths at which their kinetic measurements could be performed. The list of wavelengths chosen to monitor the substitution of the coordinated aqua ligands in these complexes is summarized in Table SI 1 (ESI†). The trial experiments also showed that all reactions were characterized by two steps, a fast step fitting the timescale of the stopped-flow reaction analyzer and a slower second step that could be studied by UV-visible spectroscopy. These reaction steps are assumed to be the substitution of the coordinated aqua ligands followed by the displacement of one of the coordinated pyridyl units in the chelate framework as previously reported.[15a,30] For

Table 2 Density functional theoretical (DFT)[21] minimum energy structures, HOMO and LUMO frontier molecular orbitals for dinuclear complexes with phenyldiamine and cyclohexyldiamine bridging fragments. The calculations were performed with the Spartan '04 for Windows quantum chemical package[22] using the B3LYP hybrid functional method[23] utilizing the LACVP+**[24] pseodopotentials basis set

Complex	bpcHna	cHn	dcHnm	bpPha	mPh	pPh	dPhm
Structure	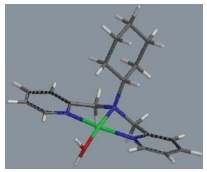	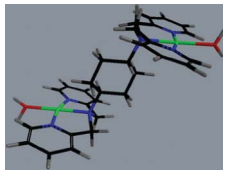	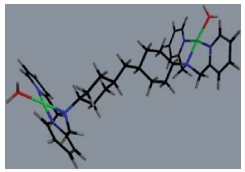	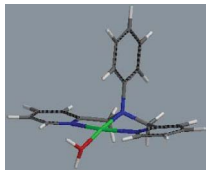	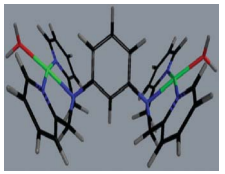	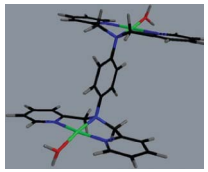	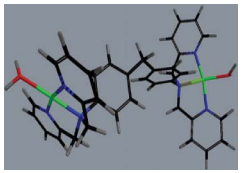
HOMO map	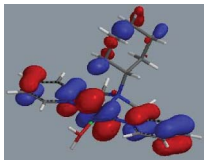	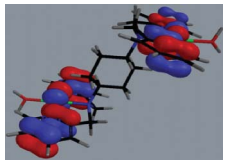	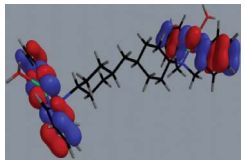	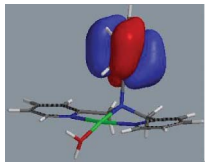	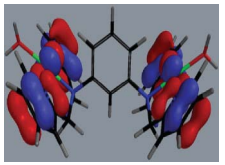	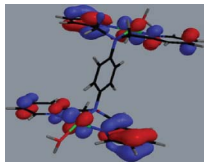	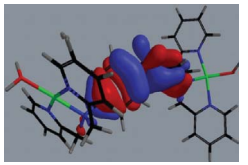
LUMO map	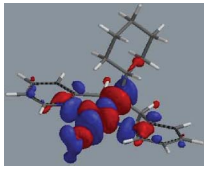	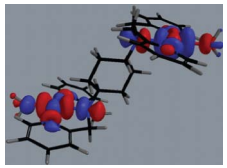	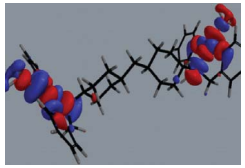	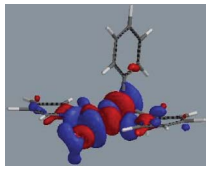	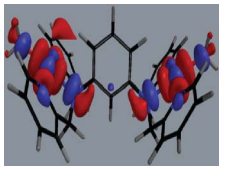	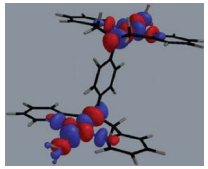	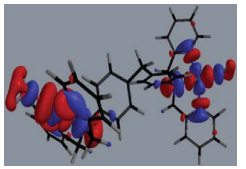

Table 3 Summary of DFT[21] computational data for the dinuclear Pt(II) complexes and their mononuclear analogues (data taken from ref. 15*a** and 15*b*[**], respectively)

Property	**bpma***	**bpha****	**bpcHna**	**cHn**	**dcHnm**	**bpPha**	**mPh**	**pPh**	**dPhm**
Bond lengths (Å)									
Pt–OH_2	2.151	2.161	2.164	2.144	2.156	2.153	2.140	2.140	2.143
Pt–N_{trans}	2.012	2.036	2.046	2.062	2.052	2.048	2.052	2.064	2.054
Separation distances (Å)									
$N_{1\ trans}$–$N_{2\ trans}$				5.99	11.30			5.99	6.54
$Pt_{1\ coord.\ plane}$–$Pt_{2\ coord.\ plane}$				8.77	14.20		3.63	8.59	10.63
Pt–$H_{proximal}$		2.99	2.79	2.87	2.79	2.62	2.65	2.72	2.76
Bond angles (°)									
N_{cis}–Pt–N_{cis}	165.8	166.5	166.8	166.9	166.8	167.7	166.4	167.0	167.4
Pt_1–$N_{1\ trans}$–$N_{2\ trans}$				119.2	38.98		105.8	118.5	
$N_{1\ trans}C_{bridge's\ central}$–$N_{2\ trans}$					143.1		125.5		134.5
Elevation angle of bridge/tail, α^a		40.8	63.2	60.8		63.4		61.5	131.3
Inclination angle of aqua ligands (relative to coord. plane)		13.60	12.51	13.36	12.11	12.92	12.51	13.36	14.39
Energy gap (eV)									
LUMO energy	−8.82	−8.51	−8.45	−10.64	−10.32	−8.53	−12.22	−12.06	−10.82
HOMO energy	−14.05	−13.75	−13.56	−15.82	−15.51	−12.92	−17.15	−17.05	−15.33
$\Delta E_{LUMO-HOMO}$	5.23	5.24	5.11	5.18	5.19	4.39	4.93	4.99	4.51
Natural charges for Pt1 and Pt2	1.215	1.206	1.203	1.220	1.215	1.215	1.231	1.226	1.221
Symmetry	C_{2h}	C_{2h}	C_{2h}	C_{2h}	C_{2v}	C_{2h}	C_{2v}	C_{2h}	C_{2v}[b]

[a] α is the supplementary angle to the angle {Pt1–N1 $_{trans}$–N2 $_{trans}$} in complexes with C_{2h} symmetry. The projection of the first coordination plane relative to the second ($Pt_{1\ coord.\ plane}$–$Pt_{2\ coord.\ plane}$) was calculated from α and the length of the linker ($N_{1\ trans}$–$N_{2\ trans}$). [b] Distorted.

the dinuclear analogues, the substitution of the two aqua ligands occurs simultaneously.

Reactions were initiated by either a pressure-driven mixing technique in which equal volumes of the complex and the nucleophile were forced into the chamber of the stopped-flow instrument or by manually mixing of equal amounts of the reagents in a tandem cuvette on the UV-visible spectrophotometer. Each reaction step was followed spectrophotometrically for more than six half-lives.

The data were fitted to a non-linear least-square procedure. Representative plots from the stopped-flow analyzer, showing only the first steps involving the reactions between **dPhm** and dmtu and for **bpcHna** with tu, are given in Fig. 3a and b, respectively.

The kinetic data for the two steps fit perfectly to separate single exponentials. The pseudo first-order rate constants, $k_{obs(1/2)}$, obtained were plotted against the concentration of the entering nucleophiles (Nu) using Origin 7.5®[31] software. The plots of the observed rate constants were found to be linearly related to the concentration of the entering nucleophiles (Nu) with negligible zero *y*-intercepts. Representative plots for the reactions between the **cHn** complex and the nucleophiles for the substitution of the aqua ligands and the opening-up of the pyridyl rings are shown in Fig. 4a and b, respectively.

Thus, the dependence of the observed pseudo first-order rate constants, $k_{obs(1/2)}$, on concentration of nucleophiles is described by eqn (1):

$$k_{obs(1/2)} = k_{2(1/2)}[Nu] \quad (1)$$

where Nu = tu, dmtu, tmtu.

The values of the second-order rate constants, k_2, which resulted from the direct attack of the thiourea nucleophiles were obtained from the slopes of these plots at 25 °C and are summarized in Tables 4 and 5 for complexes bridged by the cyclohexyldiamine and phenyldiamine fragments, respectively. Included for comparison purposes in Table 4 is the kinetic data of the reference complex, Pt(H_2O)(*N*,*N*-bis(2-pyridylmethyl)amine)](CF_3SO_3)$_2$ (**bpma**)[15a] and Pt(H_2O)(*N*,*N*-bis(2-pyridylmethyl)hexylamine](CF_3SO_3)$_2$ (**bpha**).[15b]

The dependence of the second-order rate constants on temperature were also studied in the range 15–35 °C. The thermal activation parameters for the substitution and the subsequent dechelation step ($\Delta H^{\neq}_{(1/2)}$; $\Delta S^{\neq}_{(1/2)}$) were calculated from the slopes and intercepts of the Erying plots,[32,33] respectively, as formulated in eqn (2),

$$\ln(k_2/T) = -\Delta H^{\neq}/RT + (23.8 + \Delta S^{\neq}/R) \quad (2)$$

Exemplary Erying plots are shown in Fig. 5a and b for the two reaction steps of **cHn** with nucleophiles.

The activation data from the plots are presented in Tables 6 and 7 for the cyclohexyldiamine and phenyldiamine-bridged complexes, respectively.

To understand the role of the cyclohexyldiamine and the phenyldiamine bridges on the reactivity of the dinuclear Pt(II) complexes, a comparison of their reactivities to the mononuclear Pt(II) analogues (**bpcHna** and **bpPha**) is important. If literature data of **bpma**[15a] and **bpha**[15b] are included and one focus on the substitution of the aqua ligands by tu (Table 4), the rates of substitution of the mononuclear Pt(II) complexes increase in the order **bpma**[15a] < **bpha**[15b] < **bpPha** < **bpcHna**, with approximated reactivity ratios of 1 : 1.4 : 1.7 : 1.9, respectively. The trend is understandable and demonstrates the increase in σ-inductive effects due to their pendants which leads to a ground state labilization of

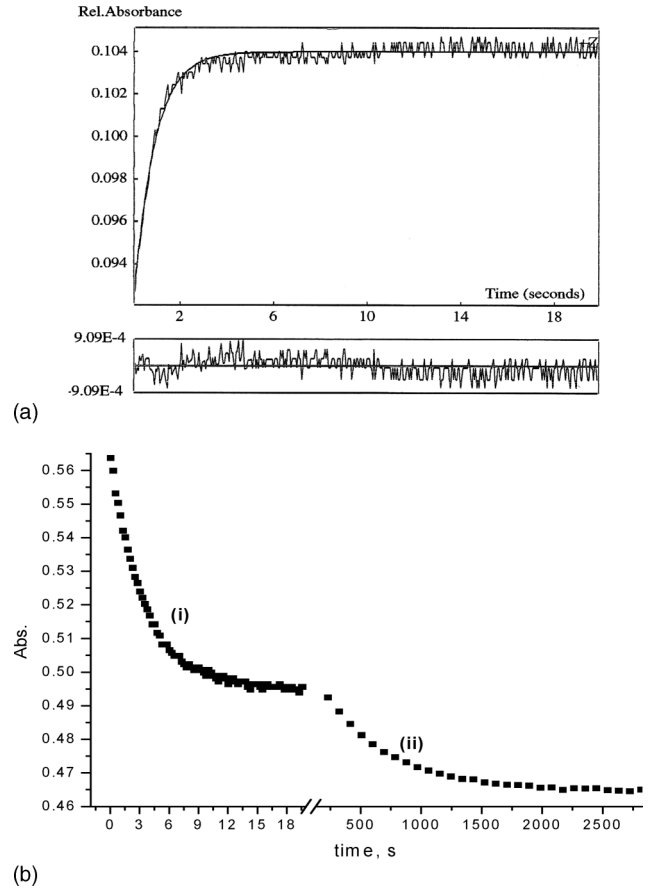

Fig. 3 (a) A typical kinetic trace from the stopped-flow acquired at 318 nm for the simultaneous substitution of the aqua ligand between **dPhm** (0.11 mM) and dmtu (6.6 mM) at 298 K, pH = 2.0, I = 0.02 M {CF_3SO_3H, adjusted with $Li(SO_3CF_3)$}. (b) A typical kinetic trace showing the two-step reaction between **bpcHna** (0.1 mM) and tu (3 mM) recorded at 284 nm, T = 298 K, pH = 2.0, I = 0.02 M {CF_3SO_3H, adjusted with $Li(SO_3CF_3)$}.

the *trans*-coordinated aqua ligand through the *trans*-influence.[15b] This is in agreement with the trend in the calculated Pt–OH_2 bond lengths which increases in the order 2.151 Å (**bpma**[15a]) < 2.161 Å (**bpha**[15b]) < 2.164 Å (**bpcHna**). An exception is **bpPha** which has a phenyl substituent.

The superior reactivity of **bpcHna** over **bpha**,[15b] an isomeric analogue with the same number of carbon atoms in its pendant extend this thinking and signifies the consequence of an intuited intra-cyclization of the hexa-carbon pendant on the general reactivity of the Pt centres. Thus, cyclization of the hexyl pendant leads to greater ground-state labilization of the *trans*-coordinated ligand of **bpcHna** *via* increased σ-donation from its cyclic pendant. The appended group in the **bpcHna** complex is bonded to the *trans*-N atom through a secondary carbon which is known to be a better σ-donor than a primary carbon, *vide supra*.[27] The inductive effects on the ground-state properties of the Pt(II) amphiphiles are further supported by computational data which show calculated HOMO–LUMO energy gaps which are lower for the two appended complexes than **bpma**.[15a] This also causes the decrease in the NBO charge on the metal centres from **bpma**[15a] (1.215) > **bpha**[15b] (1.206) > **bpcHna** (1.203). Accordingly, the frontier molecular orbitals of the appended complexes are raised in energy relative to that of

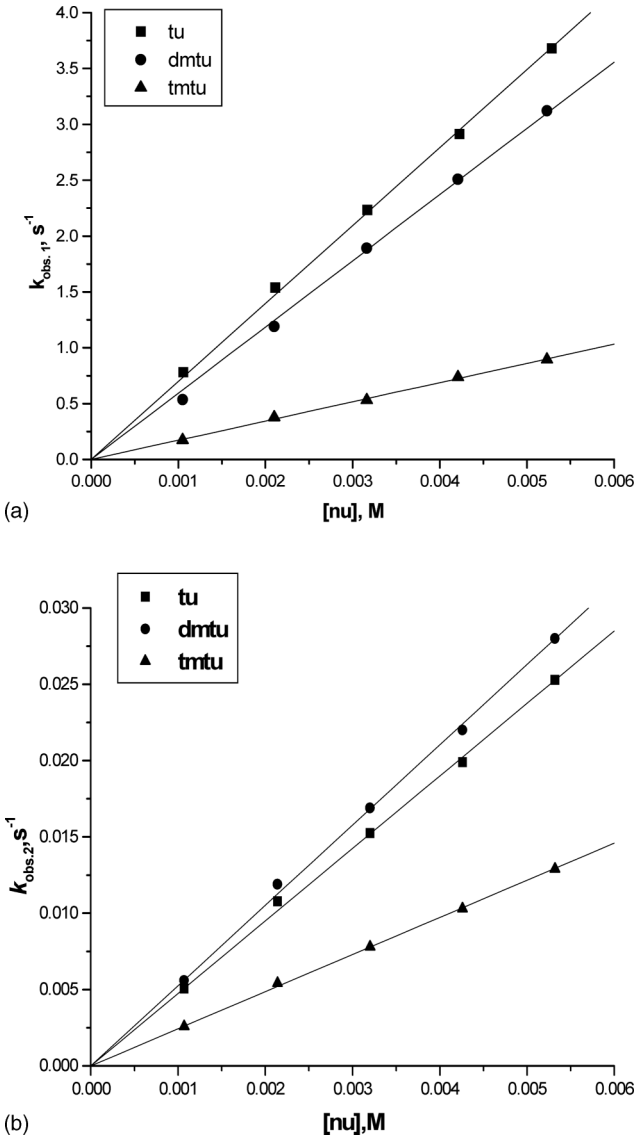

Fig. 4 (a) Concentration dependence of $k_{obs(1st)}/s^{-1}$, for the simultaneous displacement of the aqua ligands in **cHn** by thiourea nucleophiles, pH = 2.0, T = 298 K, I = 0.02 M {0.01 M CF_3SO_3H, adjusted with $Li(SO_3CF_3)$}. (b) Concentration dependence of $k_{obs(2nd)}/s^{-1}$, for the dechelation of the pyridyl units in **cHn** by nucleophiles, pH = 2.0, T = 298 K, I = 0.02 M {0.01 M CF_3SO_3H, adjusted with $Li(SO_3CF_3)$}.

bpma[15a] as a result of increasing positive inductive effects towards their metal centres.

When the rates of the simultaneous substitution of the aqua ligands of the dinuclear complexes (**cHn** and **pPh**) are compared to their respective mononuclear analogues (**bpcHna** and **bpPha**) a similar trend is observed. Using the rate constants for tu, lower rates of aqua substitutions are recorded for the respective dinuclear complexes. This is despite the increase in the total charge from +2 from the mononuclears to +4 in the dinuclears. As already pointed out, this is due to a direct consequence of the overlap geometry which enacts aerial steric influences in the dinuclear complexes. The short cyclohexyldiamine of **cHn** and the phenyldiamine of **pPh** anchor the planar Pt(II) chelates at inclination angles of 60.8 and 61.5°, respectively. The other factor which plays a role on slowing the reactions of the dinuclears is the sharing of the linker by the two

Table 4 Summary of the rate constants for the simultaneous substitution of aqua ligands ($k_{2(1st)}$) and the dechelation of one of the pyridyl units by thiourea nucleophiles ($k_{2(2nd)}$) in bis(2-pyridylmethyl)amine chelated dinuclear complexes with cyclohexyl diamine bridges and their monomeric analogue (data taken from ref. 15*a** and 15*b***, respectively).

		2nd-order rate constant/M^{-1} s^{-1}	
Complex	Nu	$k_{2(1st)}$	$k_{2(2nd)}$
bpma* (C_{2v})	tu	409 ± 2	4.95 ± 0.06
	dmtu	394 ± 1	4.05 ± 0.07
	tmtu	190 ± 0.5	2.16 ± 0.06
bpha** (C_{2h})	tu	566 ± 3	4.24 ± 0.07
	dmtu	668 ± 4	5.94 ± 0.05
	tmtu	187 ± 0.3	2.04 ± 0.01
bpcHna (C_{2h})	tu	942 ± 4	6.95 ± 0.01
	dmtu	1031 ± 6	9.56 ± 0.02
	tmtu	209 ± 1	2.18 ± 0.05
cHn (C_{2h})	tu	602 ± 9	4.75 ± 0.07
	dmtu	698 ± 6	5.26 ± 0.05
	tmtu	172 ± 2	1.63 ± 0.02
dcHnm (C_{2v})	tu	774 ± 3	7.76 ± 0.07
	dmtu	937 ± 3	8.69 ± 0.09
	tmtu	211 ± 2	2.43 ± 0.05

Table 5 Summary of the rate constants for the simultaneous substitution of aqua ligands ($k_{2(1st)}$) and the dechelation of one of the pyridyl units by thiourea nucleophiles ($k_{2(2nd)}$) in bis(2-pyridylmethyl)amine chelated dinuclear complexes with phenyldiamine bridges and their monomeric analogue

		2nd-order rate constant/M^{-1} s^{-1}	
Complex	Nu	$k_{2(1st)}$	$k_{2(2nd)}$
bpPha (C_{2h})	tu	702 ± 3	6.32 ± 0.1
	dmtu	940 ± 3	6.35 ± 0.09
	tmtu	223 ± 2	3.32 ± 0.02
mPh (C_{2v})	tu	498 ± 2	5.17 ± 0.02
	dmtu	477 ± 3	4.01 ± 0.01
	tmtu	133 ± 1	1.60 ± 0.03
pPh (C_{2h})	tu	487 ± 4	4.21 ± 0.02
	dmtu	569 ± 3	4.81 ± 0.06
	tmtu	253 ± 1	2.28 ± 0.02
dPhm (C_{2v})	tu	555 ± 4	4.65 ± 0.02
	dmtu	490 ± 5	4.84 ± 0.04
	tmtu	295 ± 2	2.64 ± 0.02

Pt metal atoms. This reduces the inductive effect experienced by each metal centre when compared with that of the mononuclears. The net effect is a reduced *trans*-influence on the leaving groups. This is supported by the DFT calculations which show an increase in the Pt–N_{trans} bond lengths from **bpcHna** to **cHn** as is true for **bpPha** to **pPh**. This is accompanied by a decrease in the Pt–OH_2 bond lengths in each respective pairs of complexes.

When a comparison between the reactivity of the two C_{2h} dinuclears (**cHn** and **pPh**) is made, **cHn** is found to be slightly more reactive than **pPh**. This is expected on the basis of a weaker σ-inductive effect due to its phenyl pendant relative to a cyclohexyl

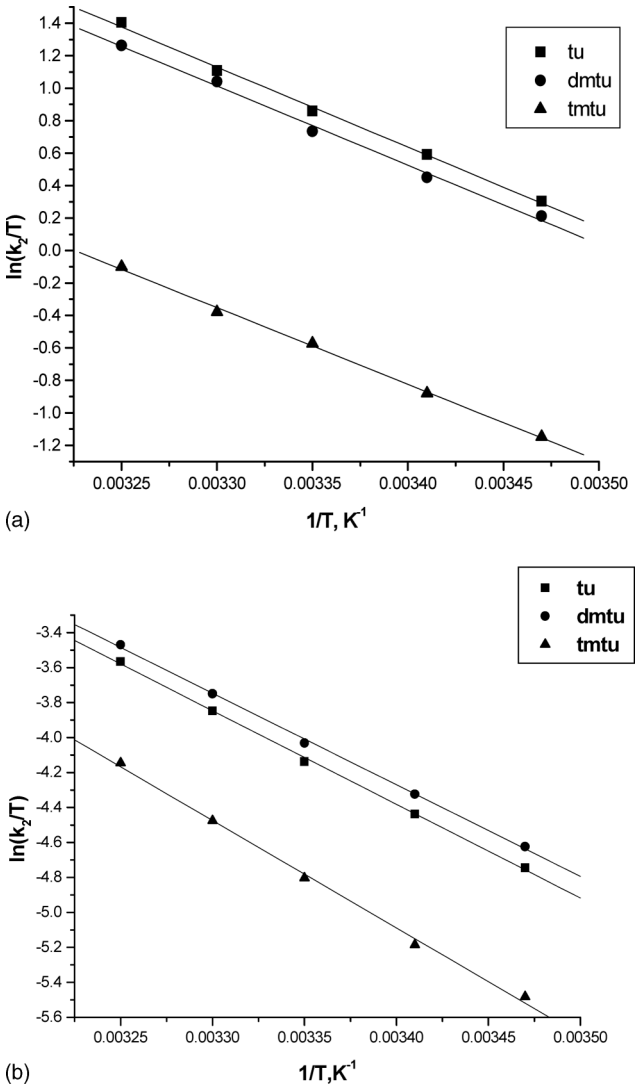

Fig. 5 (a) Temperature dependence of $k_{2(1st)}/M^{-1}$ s^{-1}, for the simultaneous displacement of the first aqua ligand in **cHn** by thiourea nucleophiles pH = 2.0, I = 0.02 M (0.01 M CF_3SO_3H, adjusted with $Li(SO_3CF_3)$). (b) Temperature dependence of $k_{2(2nd)}/M^{-1}$ s^{-1}, for the dechelation of the pyridyl units in **cHn** by thiourea nucleophiles, pH = 2.0, I = 0.02 M (0.01 M CF_3SO_3H, adjusted with $Li(SO_3CF_3)$).

pendant if the same aerial steric influences are assumed on the Pt(II) chelates of the C_{2h} dinuclears.

However, when a methylene spacer is incorporated in between the bridges of **cHn** and **pPh** the Pt, Pt distance is much increased. This also increases flexibility, resulting in structural reorganization from C_{2h} (**cHn** and **pPh**) to C_{2v} and a formation of trough-shaped molecular structures (**dcHnm** and **dPhm**). This reorganization is necessary so as to maintain an in-plane coordination of the pyridyl rings at the Pt(II) metal centres. The C_{2v} structures and their overlooking Pt(II) chelates aid the entrapment[34,35] of incoming nucleophiles in the trough-shaped dinuclears to a certain extent even though their cavities have wider basal widths. This, together with the much reduced steric hindrance on the Pt(II) chelates account for the slight increase in the reactivity from **cHn** to **dcHnm** and from **pPh** to **dPhm**. In addition, the inductive effect is also playing a role by increasing the *trans*-effect experienced by the

Table 6 Summary of the activation parameters for the simultaneous substitution of aqua ligands and the dechelation of one of the pyridyl units by thiourea nucleophiles in bis(2-pyridylmethyl)amine chelated dinuclear complexes with cyclohexyl diamine bridges and their monomeric analogue (data taken from ref. 15*a** and 15*b*****, respectively)

		Activation enthalpy/ kJ mol^{-1}		Activation entropy/ J mol^{-1} K^{-1}	
Complex	Nu	$\Delta H^{\neq}_1$	$\Delta H^{\neq}_2$	$\Delta S^{\neq}_1$	$\Delta S^{\neq}_2$
bpma* (C_{2v})	tu	41 ± 1	46 ± 0.3	−57 ± 3	−79 ± 1
	dmtu	37 ± 1	52 ± 1	−71 ± 3	−59 ± 4
	tmtu	43 ± 1	59 ± 1	−56 ± 3	−38 ± 3
bpha** (C_{2h})	tu	42 ± 1	42 ± 1	−50 ± 3	−93 ± 3
	dmtu	37 ± 1	43 ± 1	−68 ± 3	−86 ± 2
	tmtu	44 ± 1	54 ± 1	−55 ± 4	−60 ± 2
bpcHna (C_{2h})	tu	24 ± 1	42 ± 2	−106 ± 2	−86 ± 6
	dmtu	34 ± 1	45 ± 2	−75 ± 2	−76 ± 5
	tmtu	39 ± 0.4	54 ± 0.4	−64 ± 1	−59 ± 1
cHn (C_{2h})	tu	32 ± 2	41 ± 1	−53 ± 4	−83 ± 3
	dmtu	41 ± 1	41 ± 1	−55 ± 5	−84 ± 3
	tmtu	39 ± 2	51 ± 1	−44 ± 5	−66 ± 5
dcHnm (C_{2v})	tu	38 ± 1	44 ± 1	−61 ± 3	−81 ± 3
	dmtu	41 ± 0.4	41 ± 1	−57 ± 2	−90 ± 3
	tmtu	47 ± 0.3	53 ± 1	64 ± 1	−55 ± 3

aqua leaving groups. This is supported by the DFT calculations of the Pt–N_{trans} and Pt–OH_2 bond lengths, as well as in the trend of the NBO charges at the Pt metal atoms. It can be concluded that the introduction of the methylene spacers enjoining the linkers not only increases the average length of the diamine bridge but also protracts the symmetry elements within the entire complex necessary to maintain an in-plane geometry at the *N*,*N*-bis(2-pyridylmethyl)amine Pt(II) chelate headgroups. Furthermore, the reactivities of the Pt(II) centres of these two dinuclears can be considered to be independent of each other due to the longer Pt, Pt distances.

Comparing the reactivities of isomeric complexes, **pPh** and **mPh**, what is remarkable is their comparable rates of substitutions. This is despite the two complexes having DFT[21] calculated molecular structures which are completely different (Table 2), which would imply different ramifications on the lability of the coordinated aqua ligands according to the results from our previous study.[15a] One would have expected the **mPh** complex to be more reactive than either **bpPha** or **pPh** due to its bowl molecular[15a] structure and the expected entrapment of the oncoming nucleophiles. A close look at its DFT[21] optimized structure (Table 2) reveals that the sharp-edged bowl cavity formed by the overlooking coordination faces of its chelate headgroups is blocked by the phenyl ring of the 1,3-phenyldiamine bridge which intrudes into the cavity of the bowl. This is unlike in the unhindered bowl of the propyldiamne reported in our earlier work[15a] where an unusually high reactivity was recorded. This cancels out the expected entrapment[34,35] of incoming nucleophiles due to its bowl structure to a significant extent, leading to lower than expected rates of substitution. Thus, the magnitude of the steric effects mutually imposed on each equatorial coordination plane in the C_{2h} structure of **pPh** is of comparable magnitude to the steric hindrance of the intruding phenyl atoms in the C_{2v} structure of **mPh**.

A common observation in the reactivity of these complexes is a second substitution step which is less sensitive to the structural changes emanating from the linking diamino bridge. This behaviour is consistent with a substitution step involving the dechelation of one of the pyridyl units of the non-labile chelate ligand as proposed in previous studies.[15,30] The second substitution step, thus proceeds at a rate which is about two orders of magnitudes lower than that for the simultaneous displacement of the aqua ligands.[15] This is possibly due to the increased constraints in the transition states, poised on the incoming nucleophiles as they displace the coordinated pyridyl ligand at an already hindered Pt centre.[30,32,36] The presence of an unexpected second substitution in both the monomeric complexes (**bpPha** and **bpcHna**) reaffirms our proposition of the dechelation of one of the *cis*-pyridyl units of the chelate ligand from the Pt(II) metal ion.[15,30] Similar de-coordination of chelated amine ligands at a square-planar centre have been reported for Au(III),[36] Pt(II)[36] and Pd(II)[37] metal centres by sulfur-containing nucleophiles. Platinum is known to have a high propensity to form stable bonds with the soft sulfur

Table 7 Summary of the activation parameters for the simultaneous displacement of aqua ligands and the dechelation of one of the pyridyl units by thiourea nucleophiles in bis(2-pyridylmethyl)amine chelated dinuclear complexes with aromatic bridges and their monomeric analogue

		Activation enthalpy/ kJ mol^{-1}		Activation entropy/ J mol^{-1} K^{-1}	
Complex	Nu	$\Delta H^{\neq}_1$	$\Delta H^{\neq}_2$	$\Delta S^{\neq}_1$	$\Delta S^{\neq}_2$
bpPha (C_{2h})	tu	38 ± 1	47 ± 1	−64 ± 4	−77 ± 4
	dmtu	32 ± 1	43 ± 1	−80 ± 2	−86 ± 2
	tmtu	42 ± 1	52 ± 1	−61 ± 4	−70 ± 3
mPh (C_{2v})	tu	34 ± 1	32 ± 2	−78 ± 2	−124 ± 4
	dmtu	28 ± 0.2	42 ± 1	−98 ± 1	−89 ± 2
	tmtu	47 ± 1	55 ± 1	−74 ± 4	−62 ± 4
pPh (C_{2h})	tu	32 ± 1	45 ± 1	−94 ± 4	−83 ± 2
	dmtu	35 ± 1	44 ± 0.3	−76 ± 2	−85 ± 1
	tmtu	53 ± 1	52 ± 1	−74 ± 4	−85 ± 4
dPhm (C_{2v})	tu	38 ± 1	46 ± 1	−146 ± 2	−79 ± 3
	dmtu	37 ± 1	44 ± 1	−75 ± 2	−85 ± 3
	tmtu	42 ± 0.3	50 ± 0.4	−98 ± 1	−69 ± 2

nucleophilic bases than the hard and smaller nitrogen donor atom of the amine ligands.[33,38]

The reactivity of the nucleophiles reflects the steric effects in the case of tmtu, characteristic of a mechanism involving bond making in the transition state. The rates of the simultaneous substitutions of the aqua in these complexes by tmtu are about three times lower than those of either tu or dmtu. This reactivity trend is in line with the steric size of this nucleophile relative to the other two. The presence of four methyl substituents adjacent to the sulfur donor atom of this nucleophile retards its rates of approach at the Pt(II) metal centres, resulting in lower substitution rates.[39,40] When compared to the reactions involving tu and dmtu, this nucleophile causes only a marginal change in reactivity when the structural features of the dinuclear complexes are changed across the two sets of complexes. As reported in other similar substitution reactions,[28,39,40] the nucleophilicity of dmtu was found to be comparable and in some cases superior to that of tu, despite a slight increase in the steric bulkiness of this nucleophile. The σ-donation of electron density due to the two methyl groups of dmtu causes the basicity[27b] of its sulfur donor atom to increase relative to that of tu. This results in a comparable reactivity at the Pt(II) centres. The sensitivity of the substitution reactions to the steric sizes of these nucleophiles also confirms the associative nature of the activation process.[30,33] The observed trend is also true for the second substitution step that involves the dechelation of the coordinated pyridyl unit.

From the results of the temperature dependence of the second-order rate constants presented in Tables 6 and 7, all the values of the enthalpies of activation ($\Delta H^{\neq}_{(1/2)}$) are small while the values of the activation entropies ($\Delta S^{\neq}_{(1/2)}$) are large and negative. Thus, the mechanism of substitution for both steps remains associative in nature.[33]

Conclusions

This study has shown that when cyclic linkers of similar carbon numbers but of different flexibility are used to bridge the *N*,*N*-bis(2-pyridylmethyl)amine Pt(II) chelate headgroups, the rates of substitutions follows a similar trend. This is an indication that the rigidity, planarity and flexibility endowed by the diamine linkers have similar influences on the reactivity and the symmetry embodied by the complexes. In the two sets of studied dinuclear complexes, the magnitude of the steric effect depends on the average distance separating the Pt(II) centres, becoming weaker as the Pt, Pt distance is increased. Accordingly, this leads to an increase in the rates of substitutions which is also controlled by the *trans*-inductive effects due to the diamine bridges towards each Pt(II) metal centre. The relative strengths of the inductive effects depend on the hybridization of the bridging ring, with that of the cyclohexyldiamine bridging group being more effective than the phenyldiamine groups. This accounts for the relatively flexible cyclohexyldiamine set of complexes being slightly more reactive than the analogous planar, rigid and aromatic phenyldiamine complexes. The acidity of the complexes is also dependent on the length of the linker, becoming less acidic as the Pt, Pt distance increases.

In as much the same way the rigidity and planarity of the moieties within the diamine linkers have been shown to control reactivity of their Pt(II) centres, we speculate that this may translate into similar effects, leading to a rich variety of well structured DNA–Pt adducts. Such well-structured crosslinks may escape the DNA repair machinery, thereby circumventing drug deactivation.

Acknowledgements

We gratefully acknowledge financial support from the University of KwaZulu-Natal and the National Research Foundation (NRF, Pretoria). We are indebted to the Alexander von Humboldt Foundation for the kind donation of the UV-visible spectrophotometer. We thank Stephanie Hochreuther at the Institute of Inorganic Chemistry, University of Erlangen-Nürnberg, Erlangen, Germany for the assistance with elementary analysis.

References

1 V. Brabec and J. Kasparková, J., *Drug Resist. Updates*, 2005, **8**, 131.
2 (*a*) M. J. Bloemink and J. Reedijk, *Met. Ions Biol. Syst.*, 1996, **32**, 641; (*b*) M. Adams, R. P. A'Hern, A. H. Calvert, J. Carmichael, P. I. Clark and R. E. Coleman, *Br. J. Cancer*, 1998, **78**, 1404.
3 (*a*) N. Farrell, *Comments Inorg. Chem.*, 1995, **16**, 373; (*b*) N. J. Wheate and J. G. Collins, *Coord. Chem. Rev.*, 2003, **241**, 133; (*c*) H. Silva, C. V. Barra, C. F. Da Costa, M. V. De Almeida, E. T. Cesar, J. N. Silveira, A. Garneir-Suillerot, F. C. F. de Paula, E. C. Pereira-Maia and A. P. S. Fontes, *J. Inorg. Biochem.*, 2008, **102**, 767.
4 S. Komeda, G. V. Kalayda, M. Lutz, A. L. Spek, T Sato, M. Chikuma and J. Reedijk, *J. Med. Chem.*, 2003, **46**, 1210.
5 G. V. Kalayada, S. Komeda, K. Ekeda, T. Sato, M. Chikuma and J. Reedijk, *Eur. J. Inorg. Chem.*, 2003, 4347.
6 (*a*) N. J. Wheate, C. Cullinane, L. K. Webster and J. G. Collins, *Anti-Cancer Drug Des.*, 2001, **16**, 91; (*b*) D. M. Fan, X. L. Yang, X. Y. Wang, J. F. Mao, J. Ding, L. P. Lin and Z. J. Guo, *JBIC, J. Biol. Inorg. Chem.*, 2007, **12**, 677.
7 (*a*) J. Kasparková, J. Nováková, O. Vrána, N. Farrell and V. Brabec, *JBIC, J. Biol. Inorg. Chem.*, 1999, **38**, 10997; (*b*) J. Kasparková, J. Zehnulova, N. Farrell and V. Brabec, *JBIC, J. Biol. Inorg. Chem.*, 2002, **277**, 48076; (*c*) M. S. Ali, K. H. Whitmire, T. Toyomasi, Z. H. Siddik and A. R. Khokhar, *J. Inorg. Biochem.*, 1999, **77**, 231; (*d*) J. W Cox, S. J. Berners-Price, M. S. Davies, W. Barlage, Y. Qu and N. Farrell, *Inorg. Chem.*, 2000, **39**, 1710.
8 S. W. Johnson, K. V. Ferry and T. C. Hamilton, *Drug Resist. Updates*, 1998, **1**, 243.
9 F. Huq, H. Daghriri, J. Q. Yu, H. Tayyern, P. Beale and M. Zhang, *Eur. J. Med. Chem.*, 2004, **39**, 947.
10 J. Kasparková, O. Vraná, N. Farrell and V. Brabec, *JBIC, J. Biol. Inorg. Chem.*, 2004, **98**, 1560.
11 (*a*) Q. Liu, Y. Qu, R. van Antwerpen and N. Farrell, *Biochemistry*, 2006, **45**, 4248; (*b*) N. Farrell, Y. Qu and M. P. Hacker, *J. Med. Chem.*, 1990, **33**, 2179; (*c*) L. R. Kelland, B. A. Murrer, G. Abel, C. M. Giandomenica, P. Mistry and K. R. Harrap, *Cancer Res.*, 1992, **52**, 822; (*d*) P. Perego, L. Gatti, C. Caserini, R. Supino, D. Colangelo and R. Leone, *J. Inorg. Biochem.*, 1999, **77**, 59; (*e*) M. S. Davies, J. W. Cox, S. J. Berners-Price, Y. Qu and N. Farrell, *J. Am. Chem. Soc.*, 2001, **123**, 1316.
12 (*a*) Y. Zhao, W. He, P. Shi, J. Zhi, L. Qui, L. Lin and Z. Guo, *Dalton Trans.*, 2006, 2617; (*b*) X. Wang and Z. Guo, *Dalton Trans.*, 2007, 1521.
13 (*a*) A. Hofmann and R. van Eldik, *J. Chem. Soc., Dalton Trans.*, 2003, 2979; (*b*) V. M. Munisamy and D. Reddy, *Int. J. Chem. Kinet.*, 2006, **38**, 202.
14 H. Ertürk, A. Hofmann, R. Puchta and R. van Eldik, *Dalton Trans.*, 2007, 2295.
15 (*a*) A. Mambanda, D. Jaganyi, S. Hochreuther and R. van Eldik, *Dalton Trans.*, 2010, **39**, 3595; (*b*) A. Mambanda and D. Jaganyi, *Dalton Trans.*, 2011, **40**, 79.
16 A. Sato, Y. Mori and T. Lida, *Synthesis*, 1992, 539.
17 Z. Tyeklár, R. R. Jacobson, N. Wei, N. N. Murthy, J. Zubieta and K. D. Karlin, *J. Am. Chem. Soc.*, 1993, **115**, 2677.
18 H. Toftlund and S. Yde-Andersen, *Acta Chem. Scand., Ser. A*, 1981, **35a**, 575.
19 (*a*) T. Buchen, A. Hazell, L. Jessen, C. J. McKenzie, L. P. Nielson, J. Z. Pedersen and D. Schollmeyer, *J. Chem. Soc., Dalton Trans.*, 1997, 2697; (*b*) S. Foxon, J. Xu, S. Turba, M. Leibold, F. Hampel, O. Walter,

C. Wurtele, M. Holthausen and S. Schindler, *Eur. J. Inorg. Chem.*, 2007, 423.
20 (*a*) Z. D. Bugarčić, B. V. Petrović and R. Jelić, *Transition Met. Chem.*, 2001, **26**, 668; (*b*) Z. D. Bugarčić, G. Liehr and R. van Eldik, *J. Chem. Soc., Dalton Trans.*, 2002, 951.
21 (*a*) R. A. Friesner, *Chem. Phys. Lett.*, 1985, **116**, 39; (*b*) R. A. Friesner, *Annu. Rev. Phys. Chem.*, 1991, **42**, 341.
22 (*a*) A. D. Becke, *J. Chem. Phys.*, 1993, **98**, 5648; (*b*) C. Lee, W. Yang and R. G. Parr, *Phys. Rev. B*, 1998, **37**, 785.
23 (*a*) Spartan 04, Wavefunction, Inc., 18401 von Karman Avenue, Suite 370, Irvine, CA, 92612, USA; Q-Chem, Inc, The Design Center, suite 690, 5001, Baum Blvd., Pittsburgh, 15213, USA, 2004. http://www.wavefun.com/; (*b*) K. Kong, C. A. White, A. I. Krylov, C. D. Sherrill, R. D. Adamson, T. R. Furlani, M. S. Lee, A. M. Lee, S. R. Gwaltney, T. R. Adams, C. Ochsenfeld, A. T. B. Gilbert, G. S. Kedziora, V. A. Rassolov, D. R. Maurice, N. Nair, Y. Shao, N. A. Besley, P. E. Maslen, J. P. Dombroski, H. Daschel, W. Zhang, P. P. Korambath, J. Baker, E. F. C. Byrd, T. van Voorhuis, M. Oumi, S. Hirata, C. P. Hsu, N. Ishikawa, J. Florian, A. Warshel, B. G. Johnson, P. M. W. Gill and B. G. Pople, *J. Comput. Chem.*, 2000, **21**, 1532.
24 (*a*) P. C. Hariharan and J. A. Polpe, *Chem. Phys. Lett.*, 1972, **16**, 217; (*b*) P. J. Hay and W. R. Wadt, *Chem. Phys. Lett.*, 1985, **82**, 299.
25 B. Pitteri, G. Annibale, G. Marangoni, V. Bertolasi and V. Ferretti, *Polyhedron*, 2002, **21**, 2283.
26 H. Ertürk, R. Puchta and R. van Eldik, *Eur. J. Inorg. Chem.*, 2009, 1334.
27 (*a*) A. Albert and E. P. Serjant, *Ionization Constants of Acid and Bases*, Methuen, London, 1962; (*b*) P. Y. Bruice, *Organic Chemistry*, 2nd edn, Prentice Hall, New York, 1998, pp. 363–366; (*c*) M. Shmülling, D. M. Grove, G. van Koten, R. van Eldik, N. Veldman and A. L. Spek, *Organometallics*, 1996, **15**, 1384.
28 (*a*) D. Jaganyi, A. Hofmann and R. van Eldik, *Angew. Chem., Int. Ed.*, 2001, **40**, 1680; (*b*) A. Hofmann, D. Jaganyi, O. Q. Munro, G. Liehr and R. van Eldik, *Inorg. Chem.*, 2003, **42**, 1688.
29 U. Maran, H. Conley, M. Frank, A. M. Arif, A. M. Orendt, D. Britt, V. Hlady, R. Davis and P. J. Stang, *Langmuir*, 2008, **24**, 5400.
30 H. Ertürk, J. Maigut, R. Puchta and R. van Eldik, *J. Chem. Soc., Dalton Trans.*, 2008, 2759.
31 Origin$^{7.5^{TM}}$ SRO, v7.5714 (B5714), Origin Lab Corporation, Northampton, One, Northampton, MA, 01060, USA, 2003.
32 J. H. Espenson, *Chemical Kinetics and Reaction Mechanism*, 2nd edn, McGraw-Hill, New York, 1995, ch. 2 and 6.
33 M. L. Tobe and J. Burgess, *Inorganic Reaction Mechanisms*, Addison-Wiley, Longman, Ltd., Essex, 1999, pp. 30–33; 70–112.
34 R. J. Mureinik and W. Robb, *Inorg. Chim. Acta*, 1971, **5**, 333.
35 (*a*) P. W. Atkins, *Physical Chemistry*, 6th edn, Oxford University Press, Oxford, 1998, pp. 825–827; (*b*) K. J. Laidler and J. H. Meiser, *Physical Chemistry*, 3rd edn, Houghton Mifflin, Boston, MA, 1999, pp. 465–466.
36 G. Annibale, L. Cattalini and G. Natile, *J. Chem. Soc., Dalton Trans.*, 1975, 188.
37 (*a*) J. Tauben, M. Rodriguez, I. Zubiri and J. Reedijk, *J. Chem. Soc., Dalton Trans.*, 2000, 369; (*b*) E. L. M. Lempers and J. Reedijk, *Inorg. Chem.*, 1990, **29**, 217; (*c*) T. G. Appleton, J. W. Connor, J. R. Hall and P. D. Prenzler, *Inorg. Chem.*, 1989, **28**, 2030; (*d*) E. W. Abel, S. K. Bhargava and K. G. Orrell, *Prog. Inorg. Chem.*, 1984, **32**, 1; (*e*) T. Rau, R. Alsfasser, A. Zahl and R. Van Eldik, *Inorg. Chem.*, 1998, **37**, 4223.
38 F. Basolo, H. B. Gray and R. G. Pearson, *J. Am. Chem. Soc.*, 1960, **82**, 4200.
39 D. Jaganyi and F. Tiba, *Transition Met. Chem.*, 2003, **28**, 803.
40 (*a*) D. Jaganyi, F. Tiba, O. Q. Munro, B. Petrović and Z. D. Bugarčić, *Dalton Trans.*, 2006, 2943; (*b*) D. Jaganyi, K. De Boer, J. Gertenbach and J. Perils, *Int. J. Chem. Kinet.*, 2008, 809; (*c*) D. Reddy and D. Jaganyi, *Transition Met. Chem.*, 2006, **31**, 792; (*d*) D. Jaganyi, D. Reddy, J. A. Gertenbach, O. Q. Munro and R. van Eldik, *Dalton Trans.*, 2004, 299.

